Discrete Spiral and Max-Link, Complementary Tools for Vision

Walter G. $Kropatsch^{1[0000-0003-4915-4118]}$

Institute of Visual Computing and Human-Centered Technology, Virtual and Augmented Reality, E193-03, Technische Universität Wien, 1040 Austria.

krw@prip.tuwien.ac.at

Abstract. Human vision is dynamic: body, head, and eye movements change the view of the actual environment. Regions and features close to the boundary are likely to disappear while the probability in the center is high that they re-appear after the movements. We therefore exploit a re-arrangement of the pixels that orders the pixels such that the center of the image is on one end of the sequence and the boundary pixels are on the other end. A discrete spiral that connects a corner of the image with the center and contains all the pixels satisfies these constraints. In addition it is a strict total order. This order enables a max-link strategy generating efficiently a spanning forest of the image. It allows the efficient contraction for the levels of an irregular pyramid. The max-link strategy on the spiral pushes the surviving vertices geometrically towards the center of the image. We explore the properties of the proposed combination and their integration into the contrast pyramid.

Keywords: Spiral total order \cdot Max-Link strategy \cdot Irregular Image Pyramids

1 Introduction

A spiral is a frequent concept appearing also in nature: spiral galaxies, young spiral ferns, or simply hose carts¹. The Stochastic pyramid of Peter Meer [13] was the first image pyramid where the levels of the pyramid were irregular graphs instead of arrays. The selection of survivors was done by choosing the local maxima of random numbers associated with every pixel. In this way the distance between surviving vertices in the next higher pyramid level was at least two. Then all the non-surviving vertices chose one survivor in their neighborhood. If there were gaps the process was repeated for the undecided pixels until every non-survivor had a surviving neighbor. Since the random numbers are not necessarily all different, decisions at such (rare cases) enhance the influence of noise and led to different pyramidal structures although the inputs were not substantially different.

i.e., $\frac{1}{1} \text{ i.e., } \frac{1}{\text{ven.wikipedia.org/wiki/NGC_1300, }} \frac{1}{\text{ven.wikipedia.org/wiki/NGC_1300, }$

W.G. Kropatsch

2

Jolion and Montanvert extended Meer's concept in the adaptive pyramid [8] by replacing the random selection by a data-dependent adaptation of the graphs at higher pyramid levels. Also the adaptive pyramid suffers from the fact that some of the decisions are very weak and hence also influenced by noise.

In the current paper we make only a small modification to the above concepts: We replace the random numbers by a strict total order of ranks that are derived from a spiral covering the image. Experience with the total order of a column major show that pyramids with identical input always create the same structure but representative pixels of homogeneous regions tend to move towards a corner of the image [1, 3]. The spiral connects the center of the image with one of the corners by a Hamiltonian path. This allows to push vertices that represent relevant regions of the image towards the center. The center of a bounded image is more likely to re-appear in a sub-sequent view than a corner even by a slight shift of successive image captures. For the selection of survivors we use a max-link strategy that is somehow related to the principle of Peter Meer but it generates a spanning forest that can be used to construct the irregular pyramid. It also allows to adapt the structure to the image's salient regions.

We first recall the basic principles of the irregular graph pyramid (Section 2). Then the strict total order is introduced together with the max-link strategy for efficiently deriving a spanning forest (Section 3). Section 4 introduces the discrete spirals, how they can be computed from a template and how to combine them efficiently with the max-link strategy. The parallel computational complexity is addressed in Section 5. Section 6 proposes how to combine data adaptivity with the spiral total order in areas of low saliency. Section 7 reports some preliminary results with the contrast pyramid that is the first pyramid that is able to propagate high spatial frequency to the higher pyramid levels and enables top-down reconstructions which are hard to distinguish from the original images although only a few percent of the original colors are used. The Conclusion summarizes the paper and enumerates a few future research issues.

2 Recall on the Irregular Graph Pyramid

The irregular graph pyramid [10] consists of several levels of plane graphs $G_i(V_i, E_i)$, i = 0, 1, ... t where the base level G_0 is the 4-neighborhood graph of an image. The pixel values $g(v), v \in V_0$, are the attributes of the vertices V_0 . Two operations generate the higher pyramid levels: **edge contractions** and **edge removals** [4]. The operation of contracting an edge deletes the edge and one of its end points (the other "survives") while the removal of an edge deletes the edge and merges its adjacent (dual) faces. Contracting an edge has the important property of preserving the connectivity of the graph while removing an edge merges the two adjacent faces. A set of edges that are contracted with the same surviving vertex are called **contraction kernels** (**CK**). The result of contracting graph G by a contraction kernel CK is denoted by G/CK.

The concept of equivalent contraction kernels (ECK) [9] allows to combine multiple contraction kernels resulting in the same graph

$$G_n = (((G_0/CK_0)/CK_1.../CK_t) = G_0/ECK$$
 (1)

as after several successive contractions. The **receptive field** $RF(v_t) \subset V_0$ of a higher level vertex $v_t \in V_t, t > 0$, can be derived directly from the base by the $\mathrm{ECK}(v_t)$ that is a forest spanning the receptive fields of all top vertices $v_t \in V_t$. A tree is an acyclic connected graph with one less edges $T \subset E$ than vertices: |T| = |V| - 1. The receptive fields of a graph $G_t = (V_t, E_t)$ at a (top) level t > 0 partition the base vertices,

$$V_0 = \bigcup_{v_t \in V_t} RF(v_t), \tag{2}$$

the receptive fields are the connected components of the spanning forest of the base graph G_0 corresponding to the ECK.

3 Total Order and Max-Link

The ECKs of a high level of the pyramid form spanning forests of the receptive fields of the roots [9]. In regular pyramids [5] the receptive fields are determined by the position of the surviving pixel, the reduction factor (in ML² called stride) and the shape of the reduction window. In irregular pyramids they are the result of the contraction process with selected contraction kernels. This selection can be related to properties of the data and, hence, the contraction adapts to the data like in the contrast pyramid [10]. But this may, in certain cases, lead to ambiguous selections that may also be influenced by noise. A simple example are large homogeneous regions where the surviving representative vertex should be in the middle of the region. To avoid that these representative vertices are located along the boundary of the region or of the image, and disappear by small shifts of the camera, we introduce a strict total order as additional attribute of the vertices.

Definition 1 (Strict Total Vertex Order (TO)). Given a plane graph G(V, E) we define the rank of a vertex as a function $\rho: V \mapsto \mathbb{N}$ with binary relations $\rho(v)$ satisfying $\forall v \neq w \in V: \rho(v) \neq \rho(w)$.

The (strict) total order of the vertices determines unique contraction kernels and, in addition, enable a large number of independent contraction kernels that can be contracted simultaneously with low parallel complexity.

Definition 2 (Independence). Two contraction kernels CK_a and CK_b are independent if the intersection of their receptive fields $RF(CK_a) \cap RF(CK_b) = \emptyset$ is empty.

² machine learning

3.1 Deriving spanning trees and spanning forests

 $ECK \subset E_0$ are spanning forests of the base graph [9].

Definition 3. Let G(V, E) denote the plane graph and $\rho(v) : V \mapsto \mathbb{N}$ be the rank of a vertex in the TO. The local neighborhood $\Gamma(v) \subset V$ of a vertex $v \in V$ is defined by all vertices that are related by an edge in E:

 $\Gamma(v) = \{w \in V | (v, w) \in E \text{ or } (w, v) \in E\}^3$. With max-link(TO), every vertex $w \in V \setminus R_{max}$ chooses the vertex $v \in \Gamma(w) \subset V$ that has the highest rank in the TO. The link $(w, v) \in T_{\oplus}$ is then an edge of the ECK:

$$T_{\oplus} = \{(w, v) \in E | w \in V \setminus R_{max}, v = \arg\max_{u \in \Gamma(w)} \rho(u) \}.$$
 (3)

The roots $R_{max} \subset V$ of each tree of the spanning forest $T_{\oplus} \subset E$ are the local maxima of the TO (see Fig. 4a).

Proposition 1. The edges $T_{\oplus} \subset E$ computed by (3) can be computed in parallel by all vertices of the graph. The parallel complexity depends only on the degree of the vertices and NOT on the number of vertices.

4 Spirals

In polar coordinates (r, θ) an Archimedean spiral (Fig. 1(a)) can be described by the equation $r = b \cdot \theta$ with real number b. The constant parameter b controls the distance between the loops. The continuous spiral can be sub-sampled (Fig. 1(b)) with constant arc length between successive sampling points. After sub-sampling by a factor of 8 the first sampling point after the center covers nearly the complete first loop of the spiral. This creates complicated configurations around the center in all further sub-samplings. A discrete version is shown in Fig. 1(c). Choosing

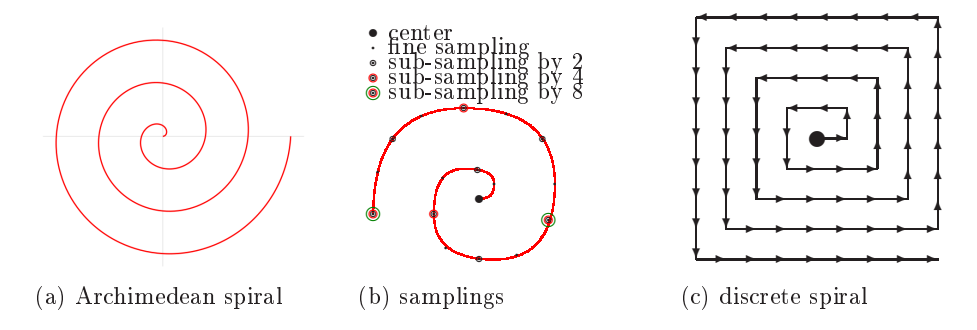


Fig. 1. Continuous to discrete spirals

b=1 the discrete spiral is image-filling i.e. covering all the pixels of the square array of the image. Pixels along the Hamiltonian⁴ path of the spiral receive an

In images 4-neighborhood is $\Gamma_4(x,y) = \{(p,q) | |x-p| + |y-q| \le 1\}$ and 8-neighborhood $\Gamma_8(x,y) = \{(p,q) | \max(|x-p|,|y-q|) \le 1\}$.

⁴ A Hamiltonian path is a path visiting every vertex of the graph exactly once.

additional attribute: This **rank** ρ measures the number of discrete steps of the path from the starting pixel.

Spirals for different images and even shapes can be cut out from a precomputed large template. Fig. 2(a) shows the onion-like relations between spirals of different sizes. Larger versions can be created without re-computing the central part and smaller versions simply remove the respective differences. Smaller sub-

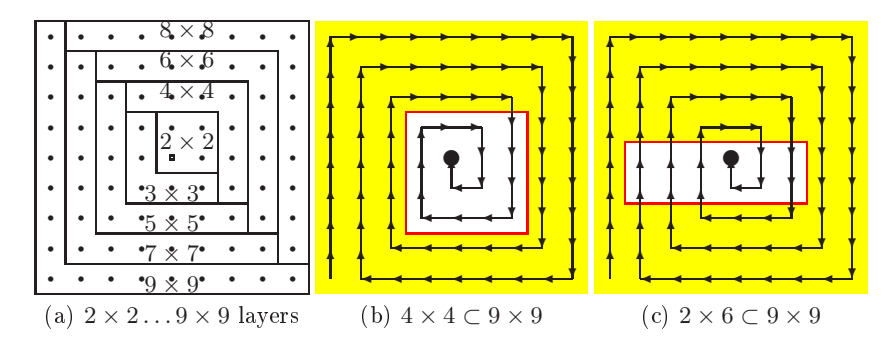


Fig. 2. Related smaller and larger sub-windows

regions can be cut out from a larger template: sub-windows as centered squares in Fig. 2(a,b). The ranks of the smaller window correspond to the ranks of the template. Centered rectangular sub-windows can also be cut out from the template (Fig. 2(c)). In these cases the ranks are no more contiguous and contain gaps. However they still form a strict total order.

Virtual links (Fig. 3) in the same orientation as the spirals of the template connect the created gaps of the 2×6 subwindow. The selected ranks in Fig. 3 are cut out from Fig. 7(b). Non-rectangular shapes can also be cut-off from the template but they may create further local extrema. Consequently the resulting ranks may form only a spanning forest. How to resolve such situations is shown in Section 6.

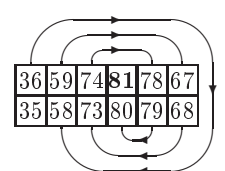


Fig. 3. Virtual links

4.1 Max-link of the Spiral Total Order

We consider now the use of the max-link strategy as defined in Def. 3 for generating a spanning forest of the image from the spiral ranks with the purpose of using the spanning forest as ECK for constructing the irregular pyramid efficiently. The 4×4 example in Figure 4 shows ranks of the spiral that start in the left lower corner ($\rho=1$) of the image, and follows the pixels along a spiral curve in clockwise order. This path is Hamiltonian and visits all vertices once.

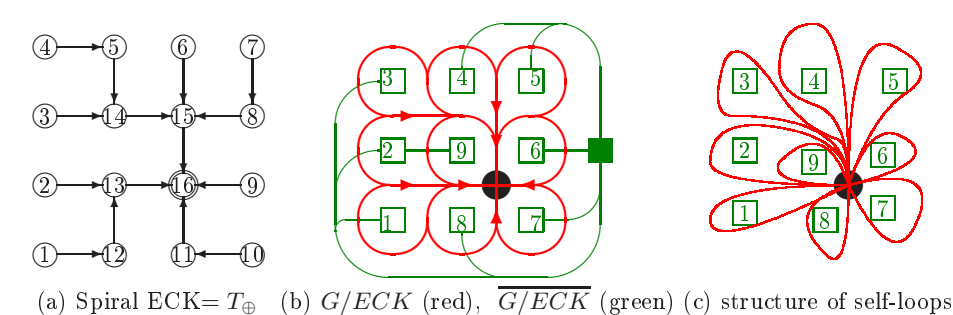


Fig. 4. 4×4 ECK of max-link of spiral

The max-links T_{\oplus} computed from the spiral are shown in Fig. 4(a) by arrows pointing towards the highest ranked 4-neighbor. It constructs the pyramid with $\mathrm{ECK} = T_{\oplus}$. The result of the contractions G/ECK is the graph $(\{\bullet\}, E_t)$ with a single vertex (Fig. 4(b)) and rank $\rho(\bullet) = 16$ in the base. The nine surviving edges form nine self-loops E_t directly attached to the root \bullet . Only the self-loop around $\boxed{2}$ includes self-loop $\boxed{9}$ in Fig. 4(c). This ECK spans the complete image if the spiral ranks are used for max-link and the branches of the spanning tree connect the root with 4-connected paths of length not longer than $\sqrt{|V|} = n = 4$ that are well suited for constructing the pyramid efficiently.

4.2 Properties of the Spanning Forests T_{\oplus}

Fig. 5 shows a 4-connected 9×9 neighborhood graph G(V, E), with $|V| = n^2 = 81, |E| = 2n(n-1) = 144$, a 9×9 discrete spiral $G_{@} = (V, E_{@}), E_{@} \subset E$ (in green). The 80 edges of the spiral cover all vertices of the image and form a Hamiltonian 4-path that connects a corner of the image with its center. The 80 maxlinks $G_{\oplus} = (V, T_{\oplus})$ are shown in red. The spiral and the max-links together contain all edges: $E_{@} \cup T_{\oplus} = E$. Both the spiral and the max-link $|E_{@}| = |T_{\oplus}| = n^2 - 1$ are trees spanning V. There are only $|E_{@} \cap T_{\oplus}| = 2(n^2 - 1) - 2n^2 + 2n = 2(n-1) = 16$ common edges (red line inside green rectangle).

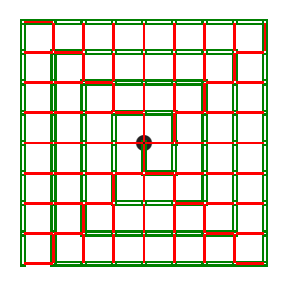


Fig. 5. Spiral and Max-links

The edges common to E_{\odot} and T_{\oplus} appear exclusively along the diagonal staircases and are independent.

Proposition 2. Let ρ denote the strict total order of the vertices of graph G(V,E) with $|V|=n^2$, $E_{\odot}\subset E$ denotes the edges of the spiral and $T_{\oplus}\subset E$ the max-links of the spiral ranks.

- In general max-link (3) produces a spanning forest SF ⊂ E of the graph G where each connected component contains one local maximum of the TO. It is the root of the tree spanning the connected component.
- 2. If we require the TO to form a slope⁵ T_{\oplus} remains connected and forms a spanning tree of the graph G with $|T_{\oplus}| = n^2 1$ links.
- 3. Independence of edges: All 4-neighbors $(v, w) \in \Gamma_4 \subset E$ of a spiral TO connect a vertex with even $\rho(v)$ and odd $\rho(w)$. Then all edges of the subset $SF_0 = \{(v, w) \in SF | \rho(v) \text{ is even}, \rho(w) \text{ is odd}\}$ are pairwise independent except at branching points of SF.
- 4. All boundary vertices are connected to one of the four diagonal stair cases of T_{\oplus} by a sequence of horizontal or of vertical edges.
- 5. orthogonality: $\forall e_{@} = (x, y) \in E_{@} \exists e_{\oplus} = (x, z) \in T_{\oplus} : e_{@} \perp e_{\oplus}$.

Proof. (Prop. 1) Every vertex $v \in V$ creates only one link to its highest neighbor. Since there are no identical ranks in the TO no cycle can be created. Any local extremum cannot link to a neighbor, following the created link backwards determines the receptive field of the extremum that is a connected component.

(Prop. 2) A slope cannot contain more than one maximum and one minimum [10, 7]. Consequently a TO that is a slope has no other extrema than the global extrema and (3) produces a spanning tree.

(Prop. 3) Since the boundary of an $m \times n$ image has always an even length 2(m+n-2) the last vertex of any loop has the opposite parity to the start vertex of the loop. This property propagates along the spiral (Fig. 4(a) and Fig. 7(b)). After contracting all vertices with even rank (except the root) only the edges with odd ranks $\rho_0 = \rho$ survive. Compacting $\rho_{i+1} = (1 + \rho_i)/2$ in $G/SF_{i+1}, i = 1, 2, \ldots$ creates again even ranks that can be contracted into their odd max-link neighbors iteratively until one root is left. The compaction of ranks reduces the number of ranks by a factor of two at each iteration and, hence, it has logarithmic parallel complexity.

(Prop. 4) Starting the spiral from a corner and incrementing the ranks along the spirals makes all ranks of the respective inner loops higher than the adjacent outer loop. Consequently max-link at vertices of the outer loop create 4-connected links to the inner loop. The only exceptions occur at the corners and when the spiral proceeds to the next inner loop.

(Prop. 5) This property is related to Property 4: links from the outer loop to the next inner loop are clearly orthogonal to the orientation of the spiral edge. Since the spiral edges at the corners form a right angle the max-link at the corners and the end-of-spiral-loop edges, the claim is satisfied.

5 Parallel Computational Complexity

Independence of edges is a pre-condition for contracting a set of edges in parallel (Def. 2). If both end points of an edge $(x, y) \in T_{\oplus}$ have degrees < 3 then the resulting (new) vertex has the lower degree of both end points, e.g. degree 1

⁵ In a slope region, every pair of vertices is connected by a monotonic path [7].

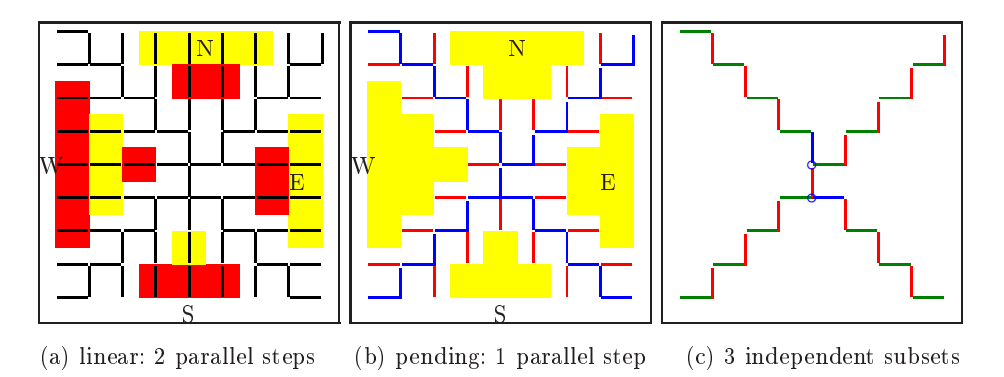


Fig. 6. Parallel steps to contract max-link of the spiral

or 2. In a linear sequence every second edge (indicated by alternating red and yellow background in Fig. 6(a)) can be contracted in parallel. The surviving edges form again a linear sequence. In this shorter sequence every second edge can be contracted again. This process reduces the length of the sequence each time by a factor of 2 until a single vertex is left.

According to Property 2.3 the 4-adjacent vertices of different spiral loops have different parity. All boundary vertices except corners and their two 4-neighbors form linear sequences until reaching either a diagonal staircase or the center (Prop. 2.4). Every linear sequence can be contracted to a single vertex by contracting repeatedly every second edge. Hence only a logarithmic number of parallel steps is needed.

What remains is shown in Fig. 6(b): there are the red pending edges and the blue diagonal staircases. Clearly all the pending edges do not share any common vertex and can be contracted in a single parallel step.

Finally the remaining staircases in Fig. 6(c) can be subdivided into following subsets of independent edges: the green horizontal edges and the red vertical edges. Two edges in the central region are colored blue because they have an end point of degree 3 (marked by a circle) in the central region where the two adjacent edges are already colored red and green. Both the green and the red subsets are independent, form linear sequences and can be contracted in logarithmic parallel steps. The remaining two blue edges need maximally two steps.

6 Combining Data Order with TO

The order of the data can be given by the different labels of connected regions as a result from a segmentation. Or it can be simply the order determined by the different grey or color values. Or the order imposed by a local brightness contrast between pixels such as used in the contrast pyramid [10]. In all these cases the order of the data may not be strict, e.g. there are pixels with the same value, label or contrast. In such cases we want to combine the order of the data with

the strict total order of the image pixels and decide on the rank inside regions of same/similar value or label based on the pre-defined total order of every pixel.

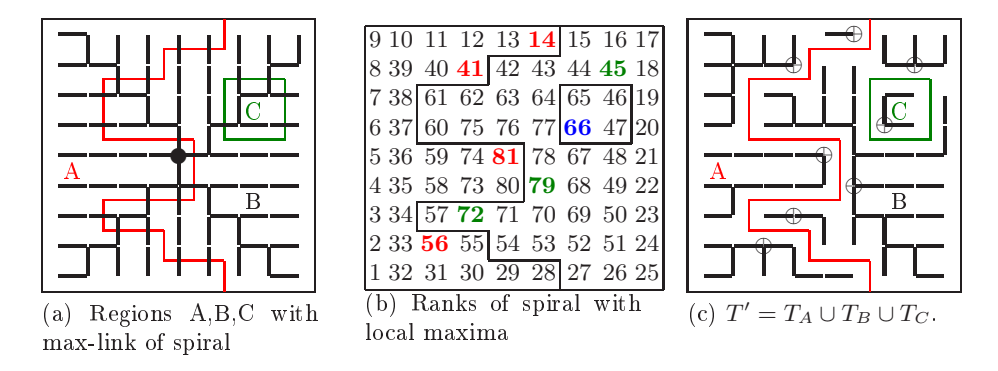


Fig. 7. Image partition into 3 regions: A,B,C

Consider a simple example: Fig. 7(a) shows a 9×9 image that is partitioned into 3 regions: $V = A \dot{\cup} B \dot{\cup} C$. The boundaries between the regions A and B are colored in red and between B and C in green. C is completely inside B. The overlay of the image with max-link of spiral in Fig. 7(b) intersects the red and green boundaries at 20 positions. Instead of removing these edges of T_{\oplus} and re-connecting the different sub-trees, we apply max-link on each of the regions A, B, C separately and get links $T' = T_A \cup T_B \cup T_C$. This may still create local maxima (\oplus) in T' and disconnect the max-links inside the regions A,B,C. Fig. 7(b,c) show 4 local maxima \oplus in A, 3 in B and one in C.

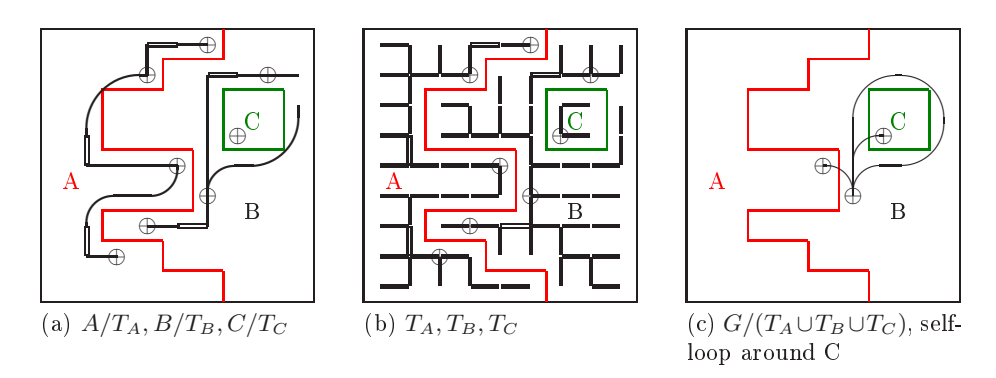


Fig. 8. Deriving the topologically correct region adjacency graph

Since the regions A,B,C are no more connected in the spanning forest T' we contract A/T_A , B/T_B , C/T_C . The surviving vertices are the local maxima of T' and the surviving edges re-connect the different components of $T_A \subset$

 $E_A, T_B \subset E_B, T_C \subset E_C$. But the connections may not be acyclic and with multiple edges. In such case we re-apply max-link on the contracted graphs $(A/T_A, E_A), (B/T_B, E_B), (C/T_C, E_C)$. Since the contracted graphs contain only the local maxima but still form a TO, the result is a spanning forest with less local maxima. The contraction of the sub-trees and re-linking with max-tree can be repeated until reaching a spanning tree for all regions⁶. Our example shows the result in Fig. 8(a) where the new connections are marked by double edges. Because the original regions are connected and contraction preserves the connectivity, the process converges to the resulting spanning trees which can be down-projected to the ECK of the original graph using the unique ranks (Fig. 8(b)). The result of contracting $G/(T_A \cup T_B \cup T_C)$ is shown in Fig 8(c). Redundant edges have been removed, the self-loop around region C is preserved. All three top vertices are at the closest position within their regions A,B,C.

General Algorithm for constructing the combined ECK

Input (Fig. 7(a,b): a) region partition $G = \bigcup_{\lambda \in \Lambda} R_{\lambda}$ with distinct labels $\lambda \in \Lambda$ for every vertex; and b) ranks ρ of the spiral TO.

- 1. For all $\lambda \in \Lambda : T_{\oplus}(\lambda) = \text{max-link of all connected regions } R_{\lambda}$.
- 2. While links of any label have more than 1 component do:
 - Re-run and re-compute max-links on R_{λ}/T_{λ} inside each region.
- 3. Expand the top spanning trees to the base following the ranks: ECK.
- 4. Contract G/ECK with the resulting ECK.
- 5. Simplify the final graph by removing redundant parallel edges and redundant self-loops.

7 Max-link with spiral TO for the Contrast Pyramid

The basic strategy (see [10] for more details) is to contract edges with increasing contrast up to a certain level that is determined by the contrast histogram [11]. In real images there are many edges with low contrast (Fig. 9(b)). Hence we use the TO of vertices to deterministically select the edges in connected regions with same contrast by the max-link of the spiral. To process several contractions in parallel one further criterium is to group edges that are independent of each other. We observed in Proposition 2 that the spiral TO provides independent subsets of edges by the parity of the ranks of the edge's end points.

Fig. 9 shows the example Fish of the Berkeley database [12] with its contrast histogram Fig. 9(b). Contrasts higher than 4 are shown in red and identify the contrast of the top level edges connecting vertices with 6% of the original colors (more examples and algorithmic details can be found in [6]). The reconstruction propagates the top colors down to the base image.

⁶ The number of repetitions is the logarithm of the longest branch in the reduced graph.

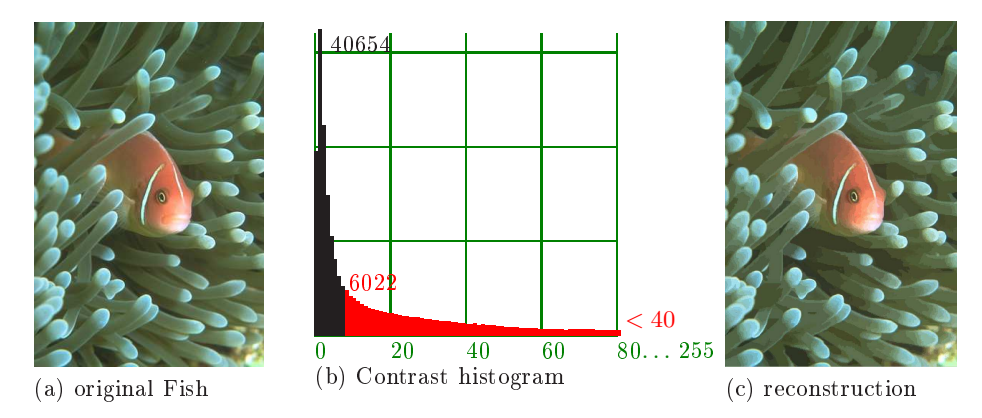


Fig. 9. Original image, contrast histogram, and reconstruction with 6% of colors

Table 1 lists the highest contrasts c_t satisfying $\sum_{c=0}^{c_t} h_0(c) < |V_0|$ for some images from the Berkeley data base [12]. All images have the same size $|V_0| = 154401$,

 $|V_t|$ is the number of vertices at the top and # crit is the number of critical points (local max, local min, sad-

top and # crit is the number of critical points (local max, local min, saddle) in the base. Therefore the mean error of the reconstructed pixels has a brightness difference smaller than 8 and 12 for images Fish and Pheasant, respectively, but is still below 30 for the other images. Empirical tests have shown (see section Gallery in [6]) that this is below the

| Berkeley# Picture | c_t | $ V_t $ | # crit |
|--------------------|-------|---------|--------|
| 210088 Fish | | 9264 | |
| 43074 Pheasant | | 4632 | |
| 160068 Cat | | 9264 | |
| 156065 Coral | | 12352 | 45915 |
| $295087~{ m arc}$ | | 12352 | |
| 55073 stone statue | 21 | | |
| 41069 squirrel | 25 | 9264 | |

noticeable deviation for human observers, that can hardly distinguish the reconstruction from the original!

8 Conclusion and Outlook

This paper proposes complementary tools for building the contrast pyramids: the spiral total order together with the max-link strategy determine the ECK for maximally contracting a given image before actually constructing the pyramid. The shown properties of the combination of the discrete spiral together with the max-link strategy not only push the surviving vertices as close as possible towards the center of the spiral, they have the potential to allow a fast parallel implementation. Since the content is actual research we expect further experimental results soon.

There is a wide range of potential applications beyond the efficient derivation of the region adjacency graph in [2]. For the computation of the max-links also the 8-neighborhood can be used. The inside of a bounding box of an image object can be linearized by a spiral and contrast-contracted as a signature of the

object. The total order for voxel images in 3D could enable efficient processing of volumetric data like CT or MRI in medical imaging.

Acknowledgments. Great thanks go to Noriane Petit and Victor Laurin who produced the experimental results with the contrast histogram during their internship in Wien, 2024-2025.

Disclosure of Interests. The author has no competing interest.

References

- 1. Banaeyan, M., Kropatsch, W.G.: Fast Labeled Spanning Tree in Binary Irregular Graph Pyramids. Jou. of Engineering Research and Sciences 1(10), 69-78 (2022).
- 2. Banaeyan, M., Kropatsch, W.G., Hladuvka, J.: Redundant 1-cells in Multi-labeled 2-Gmap Irregular Pyramids. In: Bürstmayr, H., Gronauer, A., Holzinger, A., Roth, P.M., Stampfer, K. (eds.) Proc. OAGM Workshop, Digitalization for Smart Farming and Forestry. pp. 5–22. Technische Universität Graz (September 2022).
- 3. Banaeyan, M., Kropatsch, W.G.: Adapting a Total Vertex Order to the Geometry of a Connected Component. Pattern Recognition Letters 190, 8-14 (2025).
- 4. Brun, L., Kropatsch, W.G.: Dual Contraction of Combinatorial Maps. In: Kropatsch, W.G., Jolion, J.M. (eds.) 2nd IAPR-TC-15 Workshop on Graph-based Representation. pp. 145–154. OCG-Schriftenreihe, Österreichische Computer Gesellschaft (1999), band 126
- 5. Burt, P.J.: A pyramid framework for real-time computer vision. In: Davis, L.S. (ed.) Foundations of Image Understanding, chap. 12, pp. 349-380. Kluwer (2001)
- 6. Cerman, M.: Structurally Correct Image Segmentation using Local Binary Patterns and the Combinatorial Pyramid. Tech. Rep. PRIP-TR-133, PRIP, TU Wien (2015)
- 7. Gonzalez-Diaz, R., Batavia, D., Casablanca, R.M., Kropatsch, W.G.: Characterizing slope regions. Journal of Combinatorial Optimization pp. 1–20 (2021),
- 8. Jolion, J.M., Montanvert, A.: The adaptive pyramid, a framework for 2D image analysis. Computer Vision, Graphics, and Image Processing: Image Understanding 55(3), pp.339–348 (May 1992)
- 9. Kropatsch, W.G.: Equivalent contraction kernels to build dual irregular pyramids. Adv. in Computer Science **Advances in Computer Vision**, pp. 99–107 (1997)
- Kropatsch, W.G., Banaeyan, M., Gonzalez-Diaz, R.: Controlling Topology Preserving Graph Pyramids. In: A.El-Yacoubi, M., Vincent, N., Kurtz, C. (eds.) Emerging Topics in Pattern Recognition and Artificial Intelligence, Language Processing, Pattern Recognition, and Intelligent Systems, vol. 9, chap. 2, pp. 27–76. World Scientific (2024)
- 11. Kropatsch, W.G.: Lifting some Secrets about Contrast Pyramids. In: Brun, L. (ed.) Graph-Based Representations in Pattern Recognition. submitted. (2025)
- Martin, D.R., Fowlkes, C., Tal, D., Malik, J.: A Database of Human Segmented Natural Images and its Application to Evaluating Segmentation Algorithms and Measuring Ecological Statistics. In: 8th International Conference on Computer Vision, ICCV 2001. vol. 2, pp. 416-423 (2001)
- 13. Meer, P.: Stochastic image pyramids. Computer Vision, Graphics, and Image Processing Vol. 45(No. 3), pp.269–294 (March 1989)